



POLDER2/ADEOSII, MISR, and MODIS/Terra reflectance comparisons

Pierre Lallart,^{1,2} Ralph Kahn,^{1,3} and Didier Tanré⁴

Received 29 November 2007; revised 17 April 2008; accepted 18 June 2008; published 22 July 2008.

[1] Reflectance differences among Multiangle Imaging Spectroradiometer (MISR), Moderate Resolution Imaging Spectroradiometer (MODIS)/Terra and Polarization and Directionality of the Earth's Reflectances (POLDER2) are characterized, as functions of observation geometry and spectral bands. For observations having similar geometry, corresponding normalized reflectances from MISR and MODIS fall within 3% for all bands except the MISR red band, which is higher than MODIS and POLDER2 by about 3.5%. POLDER2 and MODIS are within less than about 1% in the blue and red, 4% in the near-infrared, and 5% in the green. Generally, MISR reflectances are at the high end of the reflectance envelope, whereas POLDER2 tends to be at the low end, yielding a spread of about 5% in the red, 5% in the near-infrared, and over 7% in the green. Reflectance differences were not quantitatively corrected for instrument-to-instrument spectral band pass differences because of the uncertainties associated with such calculations. However, these uncertainties are assessed, and the envelopes can be used to bound calibration contributions to derived geophysical quantity uncertainties, including aerosol amount and type. This is of particular importance when data from the three instruments are used together in geophysical applications.

Citation: Lallart, P., R. Kahn, and D. Tanré (2008), POLDER2/ADEOSII, MISR, and MODIS/Terra reflectance comparisons, *J. Geophys. Res.*, 113, D14S02, doi:10.1029/2007JD009656.

1. Introduction

[2] Although Multiangle Imaging Spectroradiometer (MISR) [Diner *et al.*, 1998], Moderate Resolution Imaging Spectroradiometer (MODIS) [King and Greenstone, 1999] and Polarization and Directionality of the Earth's Reflectances (POLDER2) [Deschamps *et al.*, 1994] are all space-based instruments dedicated to studying Earth's atmosphere and surface, differences in the derived geophysical products can be expected, since the measurement principles and technologies are different for each instrument. MISR has multiangle capabilities, MODIS has a large swath and broad spectral range, and POLDER has a large swath, multiangle capabilities and polarization measurement capabilities, but with lower spatial resolution than MISR and MODIS.

[3] Combining the information from these instruments is an ultimate goal that would result in a very rich data set, having large spectral coverage, wide angular range, high spatial resolution, polarization information, and relatively

high radiometric accuracy, and would also allow for time-dependent calibration monitoring. Such a data set would substantially improve our ability to detect changes in atmospheric and surface optical properties. But, before using this data set, we must know how each instrument performs radiometrically when looking at the same target under the same conditions.

[4] An initial comparison between MODIS and POLDER2 derived aerosol products was presented by Gérard *et al.* [2005]. Here, we include MISR in the comparison, with the goal of quantifying the reflectance differences among these instruments for each band. Observed top-of-atmosphere (TOA) reflectances (level 1) are very sensitive to Sun and viewing geometry. MISR and MODIS/Terra are on the same platform, and we find nearly coincident orbits for Terra and ADEOSII, with POLDER2 on board, about once every 3 days. This paper presents a global comparison of near-coincident reflectances from the three instruments in pairs. With these paired instrument coincidences, we are able to perform comparisons covering a wide swath, or a large angular range along track.

2. Instrument Descriptions

2.1. POLDER

[5] The POLDER sensor, designed with the support of Laboratoire d'Optique Atmosphérique de Lille (LOA) and built by the Centre National d'Etudes Spatiales (CNES), contains a CCD matrix detector, a rotating wheel carrying polarizers and filters, and a wide field-of-view optical train.

¹Jet Propulsion Laboratory, California Institute of Technology, Pasadena, California, USA.

²Also at Laboratoire d'Optique Atmosphérique, Université des Sciences et Technologies de Lille, Villeneuve d'Ascq, France.

³Now at NASA Goddard Space Flight Center, Greenbelt, Maryland, USA.

⁴Laboratoire d'Optique Atmosphérique, Université des Sciences et Technologies de Lille, Villeneuve d'Ascq, France.

Table 1. Satellite Data Used in This Study

Date	MISR Orbit Number	POLDER2 Orbit Number	MODIS Orbit Start Time (UTC)	Julian Day
4 May 2003	17951	37002	0105	124
10 May 2003	18044	38036	1020	130
20 May 2003	18184	41002	0105	140
23 May 2003	18230	41047	0455	143
26 May 2003	18277	42036	1020	146
8 Jun 2003	18463	45047	0455	159
10 Jul 2003	18928	53046	0310	191
13 Jul 2003	18975	54035	0840	194
16 Jul 2003	19021	55023	1230	197
19 Jul 2003	19068	56012	1755	200
26 Jul 2003	19161	57046	0310	207
1 Aug 2003	19254	59023	1230	213
20 Aug 2003	19533	64011	1620	232
23 Aug 2003	19580	64057	2040	235
30 Aug 2003	19673	66034	0700	242
2 Sep 2003	19720	67023	1230	245
15 Sep 2003	19906	70034	0700	258
1 Oct 2003	20139	74034	0700	274
7 Oct 2003	20232	76011	1620	280
23 Oct 2003	20465	80011	1620	296

The geometry of the array detector and optics produces an along-track field of view of $\pm 43^\circ$, and a cross-track field of view of $\pm 51^\circ$. The instrument orbits at 802.9 km, resulting in a cross-track swath 2400 km wide. These features allow near-complete daily coverage of Earth's surface [Deschamps *et al.*, 1994]. There are nine spectral filters on the rotating wheel, covering spectral channels from 443 nm to 910 nm. For three of the nine spectral bands (443, 670, and 865 nm), polarizers have been added to the filters to assess the degree of linear polarization along with the polarization direction. A complete measurement sequence occurs every 19.6 s. Because of the motion of the satellite, a point on Earth can be viewed during 14 successive measurement sequences, providing observations from 14 different geometries. The spatial resolution of a POLDER pixel is $6 \times 7 \text{ km}^2$ at nadir. The data provided in the Level 1 product are normalized radiances.

2.2. MISR

[6] MISR flies onboard the NASA's Terra (EOS AM1) platform. The instrument is composed by nine cameras oriented along-track at different viewing angles. Four pairs of oblique cameras are oriented at $\pm 70.5^\circ$, $\pm 60.0^\circ$, $\pm 45.6^\circ$ and $\pm 26.1^\circ$, and the remaining camera is pointed at nadir. Four spectral bands are covered from 446 nm to 866 nm. As noted by Diner *et al.* [1998], the cross-track field of view and sample spacing of each pixel is 250 m for the nadir camera and 275 m for all of the off-nadir cameras. In the along-track direction, the instantaneous footprint sizes range from 214 m in the nadir to 707 m at the most oblique angles; however, the sample spacing is 275 m for all cameras. Thus, the off-nadir footprints overlap in the along-track direction. In the global viewing mode, the four nadir spectral bands and the red band in the other eight cameras are reported at full resolution, and are mapped in ground data processing to a $275 \text{ m} \times 275 \text{ m}$ grid. Prior to use in aerosol retrievals, 4×4 averaging of these pixels is performed, generating data on a grid with $1.1 \text{ km} \times 1.1 \text{ km}$ spacings. The cross-track resolution is also 1.1 km; because

of the along-track pixel overlap, the resolution is slightly larger than 1.1 km in this dimension. For the remaining off-nadir, nonred bands, the 4×4 averaging is performed on board the instrument, and these data are mapped in ground processing to the same $1.1 \text{ km} \times 1.1 \text{ km}$ grid. MISR's swath is about 400 km wide, so global coverage is obtained in 9 days [Diner *et al.*, 1998].

2.3. MODIS

[7] MODIS also flies onboard the NASA's Terra platform, and is a wide-field imager that observes Earth in 36 spectral channels at resolutions of 250 m, 500 m, and 1 km at nadir, depending on channel. The observations are made with a cross-track viewing angle range of about $\pm 55^\circ$, which leads to a 2330 km wide swath. The entire Earth surface is observed once every 2 days [King and Greenstone, 1999].

3. Data Selection

[8] Terra and ADEOSII have very similar node local passing times of 1030 LT for the descending node. As a result, nearly coincident orbits occur every 3 days. An orbit will be defined as coincident if the same point on the ground is observed by different sensors. The orbit selection is not critical for this work, because in addition, pixel selection is made, on the basis of geometrical conditions that are also related to temporal constraints. Twenty pairs of orbits were chosen during the POLDER2 lifetime (Table 1). The sinusoidal equal area projection (Samson-Flamsted) grid was used as a reference, and all the data were reprojected and averaged to this reference grid. The step is constant along a meridian, with a resolution of $1/18^\circ$ (about 6.2 km). The line and sample coordinates in the grid for a specified latitude-longitude pair are given by:

$$\text{line} = NINT[6(90 - \text{lat}) + 0.5] \quad (1a)$$

$$N_i = NINT \left[1080 \sin \left(\frac{(\text{line} - 0.5)}{18} \right) \right] \quad (1b)$$

$$\text{sample} = NINT \left[1080.5 + \left(\frac{N_i}{180} \right) \text{lon} \right] \quad (1c)$$

where lat and lon are the latitude and longitude in degrees, respectively, and NINT is the Nearest Integer function.

[9] For this study, four spectral bands are considered: 440, 560, 670 and 860 nm (Table 2). All the level 1 data are converted to normalized reflectances:

$$R = L \frac{\pi D^2}{E_0 \cos(\theta_s)} \quad (2)$$

where L is the observed radiance, D is the Earth-Sun distance in AU at observation time, E_0 is the band-specific exoatmospheric solar irradiance at 1 AU and θ_s is the solar zenith angle.

Table 2. MISR, MODIS, and POLDER2 Spectral Band Characteristics

	MISR		MODIS		POLDER2	
	λ	Bandwidth	λ	Bandwidth	λ	Bandwidth
Blue band	446.4 nm	41.9 nm	465.7 nm	18.6 nm	444.9 nm	20 nm
Green band	557.5 nm	28.6 nm	553.7 nm	19.7 nm	564.5 nm	20 nm
Red band	671.7 nm	21.9 nm	646.3 nm	47.8 nm	670.2 nm	20 nm
NIR band	866.4 nm	39.7 nm	856.5 nm	37.7 nm	860.8 nm	40 nm

[10] One pixel in this grid contains 9 (3×3) POLDER level 1 pixels or about 270 MISR or MODIS 1 km pixels at nadir. Reflectance spatial variability is calculated for the POLDER2, MISR and MODIS data falling into each pixel of the grid; pixels having reflectance standard deviation greater than 3% are rejected for this study.

[11] For all remaining pixels, we collected all the reflectance and geometrical information; the resulting data set includes all types of targets, from dark water to bright clouds. From this data set, only pixels for which the viewing zenith angles, solar zenith angles and relative azimuths less than 1° apart in absolute value between POLDER, MISR and MODIS are compared. These angular thresholds actually define the coincidence characteristics.

[12] After this selection of coincident pixels, we also performed the same atmospheric corrections as described in the Algorithm Theoretical Basis Document (ATBD) for each instrument: an ozone absorption correction for all the bands of MISR. For POLDER2 and MODIS, there is an ozone correction only for the Blue, Green and Red bands. Water vapor absorption corrections are made for MISR NIR band, POLDER2 green, red, and NIR bands, and for MODIS red and NIR bands.

[13] For MISR and MODIS, the absorption corrections are made by calculating the effective absorption optical depths ($\tau_{i,j}$, equation (3)). The water vapor amount used for the MODIS correction is derived from the level 3 daily MODIS MOD08 product. These corrections are extensively described by *Kahn et al.* [2007]

$$\tau_{i,j} = F_{i,j} \cdot A_j \quad (3)$$

A_j is the gas column amount and $F_{i,j}$ is the band specific correction factor. Here, “i” indexes the spectral band and “j” the gas type. For POLDER2, the gaseous absorption corrections are described by *Hagolle et al.* [1999]. We used the ozone column amount from closest TOMS data.

[14] We also performed a Rayleigh scattering correction for the green, red, and NIR bands for all instruments. The correction is made using the Rayleigh spectral optical depth given in the ATBDs for each sensor [*Nicolas et al.*, 2005; *Diner et al.*, 2001; *Remer et al.*, 2006], and the optical depth is evaluated for the relevant spacecraft altitude. The Rayleigh reflectance is calculated assuming the following phase function for the molecular scattering:

$$A = \frac{3}{4} (1 + \cos^2 \gamma) \quad (4)$$

where A is the molecular phase function and γ is the scattering angle.

[15] We averaged the coefficients used to correct each pixel over the whole data set; these averaged values are

summarized in Table 3. They allow us to roughly quantify the mean differences in the atmospheric corrections due to spectral band differences. A cross means that no correction is applied. These coefficients are calculated as follows:

$$coef = \frac{R_{nc}}{R_c} \quad (5)$$

[16] R_c is the corrected reflectance, R_{nc} is the uncorrected measured reflectance. The third part of Table 3 summarizes the mean Rayleigh normalized reflectances calculated and used to correct the green, red, and NIR bands. The data set for each instrument is not the same, but these mean values give the order of magnitude of the corrections.

[17] The ozone correction difference among the three instruments is always within 1%, except for the red band, where the MODIS central wavelength is lower by about 25 nm relative to POLDER2 and MISR; this shift induces about a 2% difference in the ozone correction for the red band. The water vapor absorption correction is usually 1% or less, and the correction differences never exceed 1% among the instruments.

[18] The correction for the blue band is more difficult to achieve, as we do not know a priori the kind of target considered. In order to quantify the differences that can be induced by the Rayleigh scattering among the three instruments, we ran a radiative transfer code [*Martonchik et al.*, 1998] to simulate the TOA reflectances for a pure molecular atmosphere under different conditions. To cover a wide range of realistic conditions, we ran the code over dark water and over a bright surface, both with low and high viewing zenith angles (Table 4). For the blue band, we did not perform a Rayleigh correction explicitly, since it is large and can introduce additional uncertainties. Instead, we give a general assessment of the blue band Rayleigh signal for each instrument. Over water, the Rayleigh scattering

Table 3. Coefficients Used for Gas Absorption Corrections and for the Rayleigh Scattering in the Green, Red, and NIR Bands^a

	Blue Band	Green Band	Red Band	NIR Band
<i>Mean Ozone Absorption</i>				
MISR	0.9956	0.9241	0.9632	0.9969
MODIS	0.9922	0.9282	0.9421	X
POLDER2	0.9977	0.9257	0.9693	X
<i>Mean Water Vapor Absorption</i>				
MISR	X	X	X	0.9943
MODIS	X	X	0.9861	0.983
POLDER2	X	0.989	0.9945	0.9816
<i>Mean Rayleigh Normalized Reflectance (%)</i>				
MISR	X	4.297	2.011	0.731
MODIS	X	4.476	2.417	0.767
POLDER2	X	4.855	2.416	0.804

^aA cross means that no correction is applied.

Table 4. Top of Atmosphere Rayleigh Normalized Reflectances Simulated to Quantify the Differences in the Blue Band due to the Spectral Differences^a

Instrument	VZA	Surface Type	Blue Band	Green Band	Red Band	NIR Band
MISR	10	water	0.06531	0.02657	0.01236	0.00436
MODIS	10	water	0.06473	0.02663	0.01250	0.00437
POLDER	10	water	0.06536	0.02648	0.01236	0.00436
MISR	50	water	0.07746	0.03195	0.01488	0.00523
MODIS	50	water	0.07655	0.03204	0.01516	0.00526
POLDER	50	water	0.07753	0.03178	0.01489	0.00525
MISR	10	land	0.33284	0.31678	0.31014	0.30593
MODIS	10	land	0.33832	0.31641	0.30921	0.30586
POLDER	10	land	0.33236	0.31742	0.31009	0.30589
MISR	50	land	0.34133	0.32350	0.31552	0.31023
MODIS	50	land	0.34782	0.32308	0.31454	0.31016
POLDER	50	land	0.34076	0.32422	0.31546	0.31019

^aUnit of reflectance is %. The other bands are also represented.

correction differences are very small between MISR and POLDER2, because of their close spectral response, whereas MODIS differs from 0.07 to 0.1% from MISR and POLDER2, depending on band. Over bright surfaces, MODIS differs from POLDER2 and MISR by about 0.7%.

4. Results

4.1. POLDER2-MISR-MODIS

[19] Requiring that all three instruments meet simultaneously the geometric constraints for coincident viewing reduces dramatically the number of points, and according to our thresholds, no valid coincidences have been found over the 20 orbits. So the comparison is made with pairs of instruments, and we subsequently check the consistency of the three sets of pair-wise comparisons.

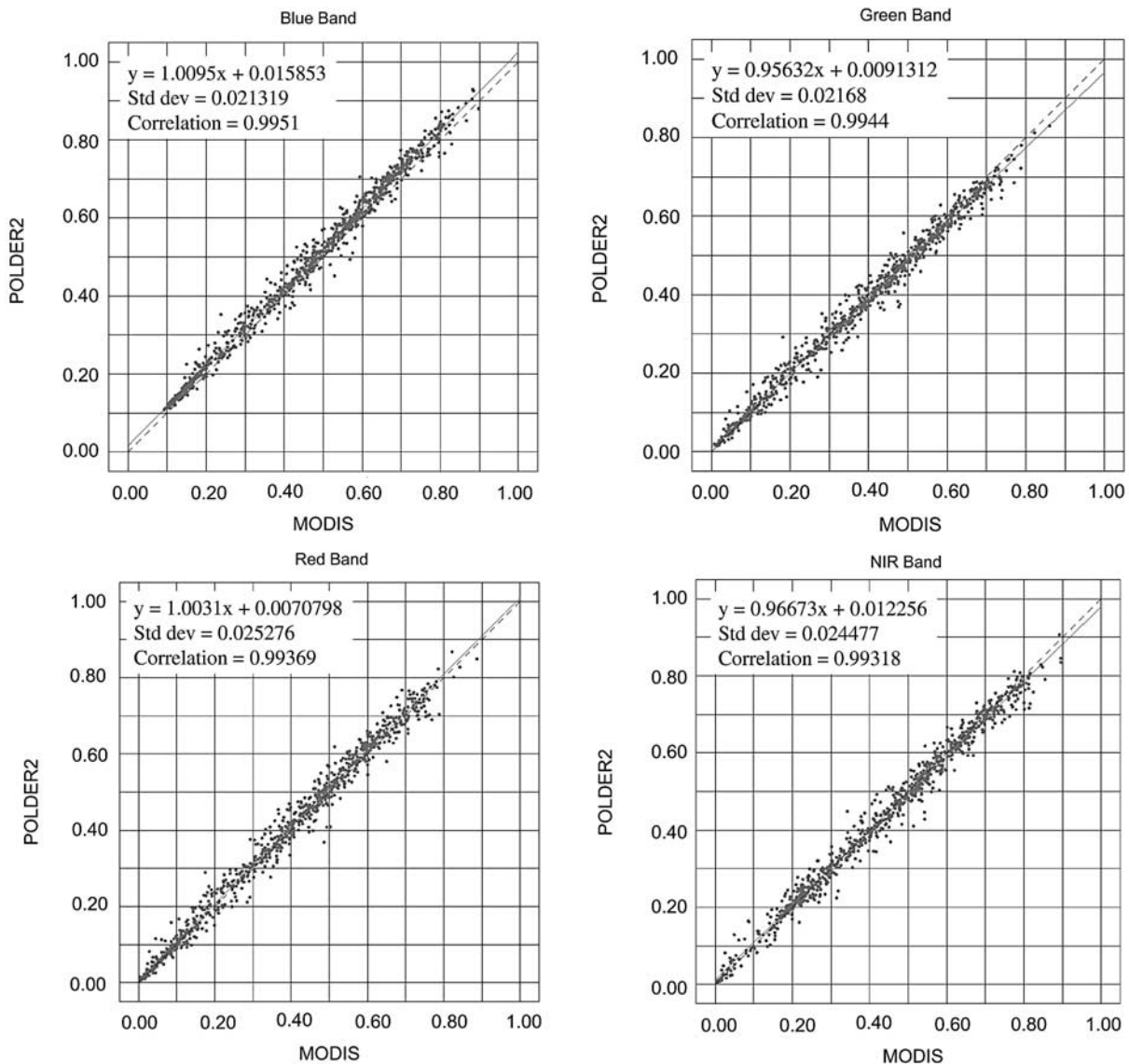


Figure 1. Nadir-view spectral reflectance comparisons between POLDER2 and MODIS for 899 coincident events, where the Sun and viewing angles for the two instruments are within 1°. (top left) Blue band, (top right) green band, (bottom left) red band, and (bottom right) near-infrared band.

Table 5. Regression Line Slopes and Offsets for the Nadir-View Spectral Comparisons Between POLDER2 and MODIS Given in Figure 1

	Blue	Green	Red	Near-Infrared
Slope	1.009	0.956	1.003	0.966
Offset	+0.016	+0.009	+0.007	+0.012

4.2. POLDER2-MODIS

[20] Although MODIS makes measurements only in the cross-track direction, POLDER2 and MODIS Terra both have wide swaths, which allows for a good number of coincident pixels; 899 cases meeting the criteria are presented in Figure 1, for each of the four spectral bands. Reflectance correlations between the two instruments are all

about 0.994. But there are systematic differences in the regression coefficients, summarized in Table 5. These may be attributed at least in part to spectral band differences (Table 2); their effects become more important as view zenith angle increases. The slope differences never exceed 4%, except in the green band. (By “slope difference,” we mean the deviation from unity of the slope of the regression line fit to the pair-wise scatterplots; this is equivalent to a difference in gain between the pair of channels.) Note that MODIS is higher than POLDER2 in the NIR (3.4%) and green (4.4%) channels, and is lower by 0.3% and 0.9% for the red and blue bands, respectively. In addition, there is an offset of 1.6% in the blue band and 1.2% in the NIR band. According to Table 4, the upper bound of the discrepancy due to blue band Rayleigh scattering is 0.7% and 0.1% for the NIR band. Since these band comparisons show very good consistency, we estimate a calibration offset lower

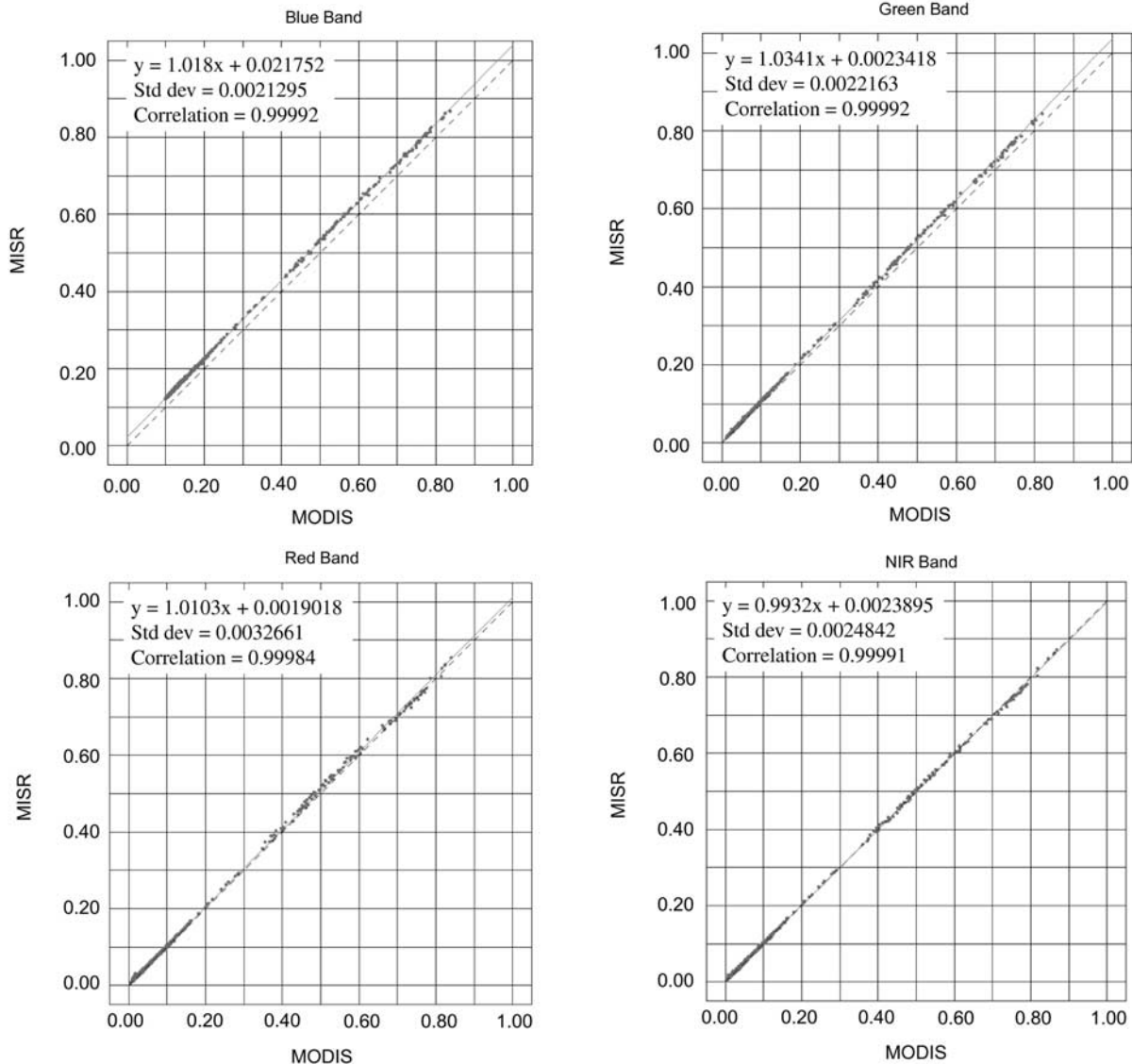


Figure 2. Nadir-view spectral reflectance comparisons between MISR and MODIS for 5648 coincident events, where the Sun and viewing angles for the two instruments are within 1°. (top left) Blue band, (top right) green band, (bottom left) red band, and (bottom right) near-infrared band.

Table 6. Regression Line Slopes and Offsets for the Nadir-View Spectral Comparisons Between MISR and MODIS Given in Figure 2, Along With Those From *Lyapustin et al.* [2007]

	Blue		Green		Red		Near-Infrared	
	Here	Lyapustin	Here	Lyapustin	Here	Lyapustin	Here	Lyapustin
Slope	1.020	1.047	1.022	1.026	1.035	1.059	0.995	1.011
Offset	+0.017	+0.015	+0.001	-0.003	+0.001	-0.003	+0.002	+0.001

bound of 0.9% for the MODIS blue band and 1.1% for the POLDER2 NIR band. For the other bands, the Rayleigh correction differences are negligible compared to the observed deviations.

4.3. MISR-MODIS

[21] As MISR and MODIS are flying on the same platform, their observing geometries are similar. So despite

the narrower MISR swath, we find 5648 coincidences in the 20 orbits considered. Figure 2 and Table 6 summarize the results. The work of *Lyapustin et al.* [2007] shows a MISR-MODIS reflectance comparison study using a different approach; their results are also reported in Table 6. The reflectance correlation between these two instruments exceeds 0.999 in all four spectral bands. The spread is very

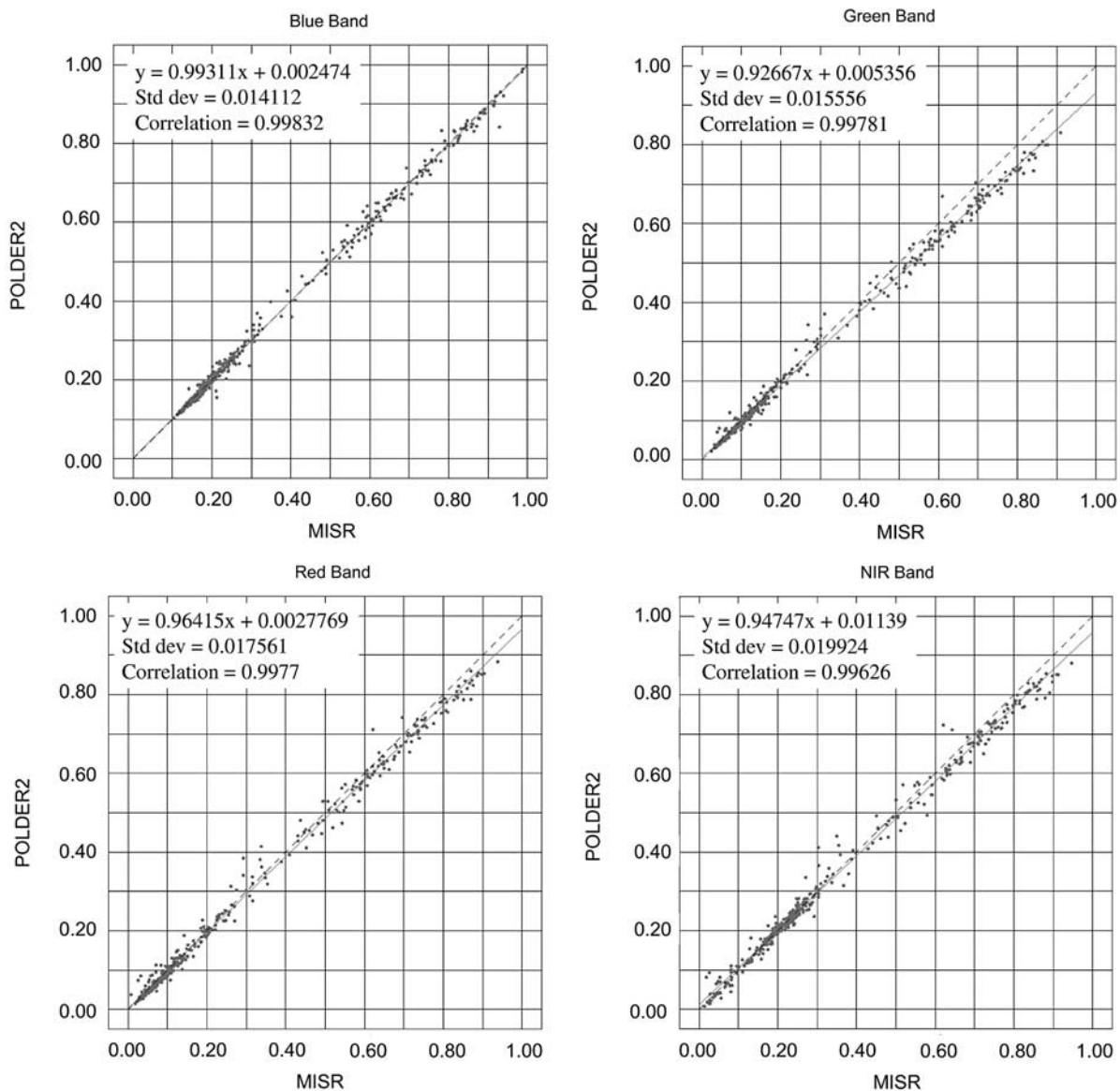


Figure 3. Multiangle along-track spectral comparisons between MISR and POLDER2 for 430 coincident events, where the Sun and viewing angles for the two instruments are within 1°. (top left) Blue band, (top right) green band, (bottom left) red band, and (bottom right) near-infrared band.

Table 7. Regression Line Slopes and Offsets for the Multiangle Along-Track Spectral Comparisons Between MISR and POLDER2 Given in Figure 3

	Blue	Green	Red	Near-Infrared
Slope	0.993	0.927	0.964	0.947
Offset	+0.002	+0.005	+0.003	+0.011

low compared to the comparisons with POLDER2 because of the lower values of the viewing angle, which cannot exceed 17° in this comparison. Except for a 3.5% slope discrepancy in the red band, the other bands agree to within 2.2% or better, and MISR is higher in all bands except the near-infrared. These results are similar to those of *Lyapustin et al.* [2007], who showed average slope differences of 2.6% and 1.1% for the green, and near-infrared bands, respectively. The blue band presents a slope difference of 4.7%, and a relatively large offset in both studies, similar to that found in the POLDER2-MODIS comparison.

[22] Again, although the MISR and MODIS bands are not exactly similar spectrally (Table 2), differences in the spectral band passes are not fully accounted for in these comparisons. In particular, the (unknown) surface spectral characteristics are not accounted for in the statistical approach taken here. However, the results of *Lyapustin et al.* [2007] are within one percent of those obtained here for the green and near-infrared bands, and within two percent for the blue and green bands, despite differences in the data selected and the approach used, including spectral band pass corrections that were attempted in that study. The similarity of results supports our key conclusions, especially for the outliers (e.g., the MISR red band), which exhibit discrepancies exceeding by factors of two the differences between the results of these two studies.

4.4. POLDER2-MISR

[23] Despite the narrow MISR swath, 430 pixels coincident with POLDER2 that meet the acceptance criteria were found in the 20 orbits. The results are presented in Figure 3 and Table 7. Correlations are all greater than 0.996. The blue band comparison is very good, due in part to the similarity of the blue band spectral response. Generally, MISR is at the high end of the reflectance comparison envelope for the three instruments, whereas POLDER2 is at the low end. There is a consistent slope difference of about 5% for the NIR band and about 3.5% for the red band, whereas the blue band is in near-perfect agreement. As with the MODIS comparison, the green band is an outlier, with POLDER2 biased low by 7.3%. For the NIR band, we also

see the same 1.2% offset as in the POLDER2-MODIS comparison.

5. Conclusions

[24] Establishing the envelopes of reflectance differences is a necessary first step in comparing and ultimately combining geophysical products from MISR, MODIS, and POLDER2. We performed spectral reflectance comparisons among the three instruments, controlling for Sun and viewing geometry as well as scene heterogeneity. No attempt was made here to correct for spectral band differences due to the uncertainties such calculations introduce; the magnitudes of these corrections are relatively small, as demonstrated in recent studies in which such corrections were attempted [*Lyapustin et al.*, 2007; *Kahn et al.*, 2005, 2007]. We did perform ozone and water vapor corrections, and established bounds on the magnitude of Rayleigh scattering differences, since these can be performed reliably, and they have significant, systematic effects on the observed reflectances. Our conclusions are circumscribed by these uncertainties.

[25] Generally, MISR is at the high end of the reflectance comparison envelope for the three instruments, whereas POLDER2 and MODIS are generally at the low end, though the results vary in detail with spectral band. On average, MISR and POLDER2 differ by about 5% for the NIR band, MISR is 3.5% higher in the red band, the blue band is in near-perfect agreement, and the green band is an outlier, with a slope difference of 7.3%. POLDER2 also has a 1.2% positive offset in the NIR band. MISR is higher in all cases. MISR-MODIS comparisons fall within 3% for all but the red band, in agreement with previous studies. Two bands fall outside the 3% to 5% reflectance difference envelopes: the MISR red band is high compared to both MODIS and POLDER2, and the POLDER2 green band is low compared to both MISR and MODIS. MODIS has a 1.5% negative offset in the blue band.

[26] As the data sets used in the three pair-wise comparisons are different, we can cross check the accuracy and the validity of the observed trends. We divided the trend found in the POLDER2-MODIS comparison by the trend found in the MISR-MODIS comparison and compared that result with the trend found in the POLDER2-MISR comparison; the results are shown in the Table 8. Except for the NIR band, the results differences are within 1%, and demonstrate the consistency of the method to this degree of accuracy.

[27] The results of this study can be used to assess the contributions of spectral reflectance differences to geophysical quantities derived from the three instruments, which in turn will facilitate joint application of the geophysical data

Table 8. Cross Comparison of the Trends Found in the Three Comparisons^a

	POLDER2-MODIS	MISR-MODIS	POLDER2-MISR	Calculated POLDER2-MISR
Blue band	1.009	1.020	0.99311	0.989
Green band	0.956	1.022	0.92667	0.935
Red band	1.003	1.035	0.964	0.969
NIR band	0.968	0.995	0.947	0.972

^aThe “Calculated POLDER2-MISR” column is the ratio of the slope found in the POLDER2-MODIS comparison and the slope found in the MISR-MODIS comparison.

sets. However, possible differences in the aerosol products derived from POLDER-2 cannot be attributed to the green channel calibration issue, since it is not used in the POLDER-2 standard aerosol retrieval algorithm. Also note that the observed radiometric differences, though they must be considered when applying satellite-derived geophysical quantities to cutting edge problems, are quite small compared to those for previous generations of satellite imagers.

[28] **Acknowledgments.** We thank Anne Leifermann and Jean-Luc Deuze for their support of this project. The work of P. Lallart is funded by the Centre National d'Etudes Spatiales and hosted by the Jet Propulsion Laboratory. The work of R. Kahn is supported in part by NASA's Climate and Radiation and Atmospheric Composition Research and Analysis Programs, under H. Maring and P. DeCola, respectively, and in part by the EOS-MISR instrument project. The POLDER2 data were obtained from the ICARE center (<http://www.icare.univ-lille1.fr>), the MISR data came from the NASA Langley Research Center Atmospheric Sciences Data Center (<http://www.larc.nasa.gov>), and the MODIS data were obtained from the Atmosphere Archive and Distribution System (<http://ladsweb.nascom.nasa.gov>).

References

- Deschamps, P. Y., F. M. Bréon, M. Leroy, A. Podaire, A. Bricaud, J. C. Buriez, and G. Sèze (1994), The POLDER mission: Instrument characteristics and scientific objectives, *IEEE Trans. Geosci. Remote Sens.*, *32*, 598–615, doi:10.1109/36.297978.
- Diner, D. J., et al. (1998), Multiangle Imaging Spectroradiometer (MISR) description and experiment overview, *IEEE Trans. Geosci. Remote Sens.*, *36*, 1072–1087, doi:10.1109/36.700992.
- Diner, D. J., et al. (2001), MISR level 2 aerosol retrieval algorithm theoretical basis, *JPL D11400*, rev. E, Jet Propul. Lab., Pasadena, Calif.
- Gérard, B., J.-L. Deuzé, M. Herman, Y. J. Kaufman, P. Lallart, C. Oudard, L. A. Remer, B. Roger, B. Six, and D. Tanré (2005), Comparisons between POLDER 2 and MODIS/Terra aerosol retrievals over ocean, *J. Geophys. Res.*, *110*, D24211, doi:10.1029/2005JD006218.
- Hagolle, O., P. Goloub, P.-Y. Deschamps, H. Cosnefroy, X. Briottet, T. Bailleul, J.-M. Nicolas, F. Parol, B. Lafrance, and M. Herman (1999), Results for POLDER in-flight calibration, *IEEE Trans. Geosci. Remote Sens.*, *37*, 1550–1566, doi:10.1109/36.763266.
- Kahn, R., et al. (2005), MISR low-light-level calibration, and implications for aerosol retrieval over dark water, *J. Atmos. Sci.*, *62*, 1032–1062, doi:10.1175/JAS3390.1.
- Kahn, R., M. Garay, D. Nelson, K. Yau, M. Bull, B. Gaitley, J. Martonchik, and R. Levy (2007), Satellite-derived aerosol optical depth over dark water from MISR and MODIS: Comparisons with AERONET and implications for climatological studies, *J. Geophys. Res.*, *112*, D18205, doi:10.1029/2006JD008175.
- King, M. D., and R. Greenstone (Eds.) (1999), *EOS Reference Handbook: A Guide to NASA's Earth Science Enterprise and the Earth Observing System*, NASA Doc. NP-1999-08-134-GSFC, 361 pp.
- Lyapustin, A., Y. Wang, R. Kahn, J. Xiong, A. Ignatov, R. Wolfe, A. Wu, B. Holben, and C. Bruegge (2007), Analysis of MODIS-MISR calibration differences using surface albedo around AERONET sites and cloud reflectance, *IEEE Trans. Geosci. Remote Sens.*, *107*, 12–21, doi:10.1016/j.rse.2006.09.028.
- Martonchik, J. V., D. J. Diner, R. Kahn, M. M. Verstraete, B. Pinty, H. R. Gordon, and T. P. Ackerman (1998), Techniques for the Retrieval of aerosol properties over land and ocean using multiangle data, *IEEE Trans. Geosci. Remote Sens.*, *36*, 1212–1227, doi:10.1109/36.701027.
- Nicolas, J. M., P. Y. Deschamps, H. Loisel, and C. Moulin (2005), POLDER-2/Ocean Color Atmospheric correction algorithms, *Ref. VI.1*, Lab. d'Opt. Atmos., Lille, France.
- Remer, L. A., D. Tanré, and Y. J. Kaufman (2006), Algorithm for remote sensing of tropospheric aerosol from MODIS: Collection 5, *Ref. ATBD-MOD-02*, NASA Goddard Space Flight Cent., Greenbelt, Md.

R. Kahn, NASA Goddard Space Flight Center, Greenbelt, MD 20771, USA. (ralph.kahn@nasa.gov)

P. Lallart and D. Tanré, Laboratoire d'Optique Atmosphérique, Université des Sciences et Technologies de Lille, F-59655 Villeneuve d'Ascq, France.